

Quasinormal ringing of regular black holes in asymptotically safe gravity: the importance of overtones

R. A. Konoplya,^{1,*} A. F. Zinhailo,^{1,†} J. Kunz,^{2,‡} Z. Stuchlík,^{1,§} and A. Zhidenko^{3,¶}

¹*Research Centre for Theoretical Physics and Astrophysics,
Institute of Physics, Silesian University in Opava,
Bezručovo náměstí 13, CZ-74601 Opava, Czech Republic*

²*Institute of Physics, University Oldenburg, D-26111 Oldenburg, Germany*

³*Centro de Matemática, Computação e Cognição (CMCC), Universidade Federal do ABC (UFABC),
Rua Abolição, CEP: 09210-180, Santo André, SP, Brazil*

The asymptotically safe gravity is based on the idea that the main contribution to the Schwarzschild-like black hole spacetime is due to the value of the gravitational coupling which depends on the distance from the origin and approaches its classical value in the far zone. However, at some stage this approach has an arbitrariness of choice of some identification parameter. The two cases of identification are considered here: first, by the modified proper length (the Bonanno-Reuter metric), and second, by the Kretschmann scalar (the Held-Gold-Eichhorn metric, which coincides, up to the redefinition of constants, with the Hayward metric). Even though the quasinormal modes of these metrics have been extensively studied, a number of interesting points were missed. We have found that quasinormal modes are qualitatively similar for both types of identification. The deviation of the fundamental mode from its Schwarzschild limit may be a few times larger than it was claimed in the previous studies. The striking deviation from the Schwarzschild limit occurs for overtones, being as large as hundreds of percent even when the fundamental mode is almost coinciding with the Schwarzschild one. This happens because the above metrics are very close to the Schwarzschild one everywhere, except a small region near the event horizon, which is crucial for overtones. The spectrum of both metrics contains purely imaginary (non-oscillatory) modes, which, for some values of parameters, can appear already at the second overtone.

PACS numbers: 03.65.Pm,04.30.-w,04.70.Bw

I. INTRODUCTION

Construction of the model of a quantum corrected black hole is important not only as a particular strong-gravity solution within, yet an unknown, non-contradicting quantum gravity, but also because of the fundamental problem related to the final stage of Hawking evaporation and central singularities of classical solutions. One of the approaches to this problem consists in the supposition that the gravitational coupling depends on the energy scale under consideration [1–5]. Within this approach one has to integrate the beta function for the gravitational coupling and find the Newton constant as a function of some energy scale k . Then, this energy-dependent Newton constant is used in the classical black hole solution in order to obtain the quantum corrected lapse function, describing a regular black hole [6, 7]. Actually, the idea of energy dependence of the laws of physics at the level of the action is usual for quantum field theory. After all, there are indications that the well-known AdS/CFT correspondence might emerge from the above asymptotically safe gravity [8].

Further, the gravitational coupling depends on some arbitrary renormalization scale k , so that the relation connecting the energy and the radial coordinate must be defined in order to write down the resulting quantum corrected black hole metric. At this stage we are aware of two opportunities for the identification of the parameter k :

- with the modified proper distance, resulting in the so-called Bonanno-Reuter black hole metric [6], and
- with a power of the Kretschmann scalar [4, 7, 9], leading to the Held-Gold-Eichhorn metric [7].

The latter coincides, up to the redefinition of constants, with the Hayward metric [10], which was suggested as a toy-model solution of the singularity problem within the collapse and evaporation scenario. A self-consistent deduction of the quantum corrected black hole metric with the help of the renormalization group approach was suggested by Kazakov and Solodukhin in [11], and the quasinormal modes and grey-body factors were analyzed for this case in [12, 13]. However, the Kazakov-Solodukhin solution is not free of singularity, but moves it to a finite distance from the center.

One of the basic characteristics of black holes, which depend only on the parameters of the background and not on the way of perturbations, are quasinormal modes [14, 15]. They dominate in the decay of perturbations at late times and, therefore, are observed by gravitational interferometers [16–18]. Nevertheless, the uncertainty in the

* roman.konoplya@gmail.com

† antonina.zinhailo@physics.slu.cz

‡ jutta.kunz@uni-oldenburg.de

§ zdenek.stuchlik@physics.slu.cz

¶ olexandr.zhydenko@ufabc.edu.br

angular momentum and mass of the observed black holes leaves a wide window for modified theories of gravity [19].

By now quasinormal modes of various regular black hole models have been extensively studied in a great number of papers [20–36]. Even though quasinormal modes of the relatively new Held-Gold-Eichhorn spacetime have not been studied yet, there is an extensive literature on the spectrum of the Hayward solution [33–37] the data for which could be simply re-scaled. Quasinormal modes of the Bonanno-Reuter black hole have been studied in [38–40] and of its approximate, truncated version in [41]. However in all the above studies a number of the crucial and, in our opinion, most interesting, properties of quasinormal spectra were missed for both cases.

First of all, the observed effect of quantum correction upon the fundamental mode reported in [38] for the Bonanno-Reuter metric amounted to only a few percent. However, the analysis in [38] does not include the whole parametric range and here we will show that the actual effect can be more than three times larger, exceeding 20 percent for the extremal black hole configuration.

The most interesting behavior takes place for the overtones, which was also missed in the previous papers. Although it is believed that the major contribution to the signal is owing to the fundamental mode, recently it has been shown in [42] (and later studied in [43, 44]) that up to ten first overtones are necessary in order to model the ringdown of accurate numerical relativity simulations at all times and not only at the last stage. This finding indicated also that the actual quasinormal ringing starts earlier than expected. The main motivation of the renormalization group approach considered here is certainly related to quantum corrections, which are supposed to be small for astrophysical black holes. However, as the Held-Gold-Eichhorn metric coincides also with the Hayward solution, so that our finding may have broader interpretation, including large black holes and the aspects of the overtones' behavior might be useful. In addition, we will argue that some of the features found here must be generally appropriate to a quantum corrected black hole.

Here we will show that overtones for the above regular black holes have two peculiarities: First, there are purely imaginary modes in the spectra of both black holes. These non-oscillatory modes occur already at the second overtone and therefore may affect the ringdown at earlier times. Another interesting property is the high sensitivity of overtones to the near horizon asymptotic, which leads to enormous (up to hundreds of percent) deviation of the overtones' real parts from their Schwarzschild limit, while the fundamental mode deviates from its classical limit by (at most) a few percent. In other words, in the regime when the geometry of the quantum corrected black holes is very close to the Schwarzschild one everywhere except a small region near the event horizon, the overtones differ a lot from their Schwarzschild analogues.

Here we will give a systematic analysis of quasinormal ringing (including the overtones' behavior) of the above

two regular black hole solutions for the test scalar, electromagnetic, and Dirac fields.

The analysis of gravitational perturbations for these vacuum solutions of the Einstein equation, could, in principle, be formally considered here as well. However, the main supposition of the renormalization group approach is that the dominant correction to the background metric is due to the running gravitational coupling, what implies the existence of other correction terms which were neglected. Under this supposition there is no evidence that small perturbations of the black hole background spacetime will be still much smaller than the unknown terms we initially neglected in the background. In addition, we know that gravitational perturbations are usually qualitatively similar to those for test fields and frequently coincide with the latter in the high frequency (eikonal) regime.

Our paper is organized as follows: In sec. II we give the basic information on the quantum corrected black hole metrics under consideration. Sec. III is devoted to the wave-like equation for the scalar, electromagnetic, and Dirac equations. In sec. IV we briefly review the Wentzel–Kramers–Brillouin (WKB), time-domain integration, and Frobenius methods used for calculations of quasinormal modes. In sec. V the quasinormal ringing, overtones and time-domain profiles are analyzed for both metrics and the analytical formula for quasinormal frequencies is deduced for the eikonal (high multipole number) regime. Finally in sec. VI we summarize the obtained results and discuss some open problems.

II. RENORMALIZATION GROUP-IMPROVEMENT FOR BLACK HOLE SOLUTIONS

The improved Schwarzschild metric starts from the average (ghost-free) Einstein-Hilbert action in the four dimensional spacetime [6]:

$$\Gamma_k[g_{\mu\nu}] = \frac{1}{16\pi G(k)} \int d^4x \sqrt{\det(g_{\mu\nu})} \left(-R(g_{\mu\nu}) + 2\bar{\lambda}(k) \right).$$

The scale-dependent couplings are described by the Wetterich equation

$$k \cdot \partial_k \Gamma_k = \frac{1}{2} \text{Tr} \left(\frac{k \cdot \partial_k \mathcal{R}_k}{\Gamma_k^{(2)}[\phi] + \mathcal{R}_k} \right), \quad (1)$$

where $\Gamma_k^{(2)}$ stands for the Hessian of Γ_k with respect to $g_{\mu\nu}$, and \mathcal{R}_k is a filtering function which implements the infrared cutoff, as was pointed out in Ref. [6]. In the simplest case one considers a field $\phi(x)$ defined on a Euclidean spacetime with metric $g_{\mu\nu}$.

Following [6], the evolution of the dimensionless gravitational coupling is described by the following equation

$$k \frac{d}{dk} k^2 G(k) = \left[2 + \frac{B_1 k^2 G(k)}{1 - B_2 k^2 G(k)} \right] k^2 G(k), \quad (2)$$

where B_1 and B_2 are some factors. Here we assume that the dimensionless running cosmological constant

$$\lambda = \bar{\lambda}/k^2 \ll 1$$

for all scales of interest, so that we may approximate $\lambda \approx 0$ in the arguments of $B_1(\lambda)$ and $B_2(\lambda)$.

Integrating the equation (2), one can find the Newton's coupling

$$G(k) = \frac{G_0}{1 + \tilde{\omega}G_0k^2}, \quad (3)$$

where $\tilde{\omega}$ is a constant.

From the above relation we can see that the effects of quantum corrections are essential at high energies and at the low ones the classical solution is reproduced. The next step in the procedure is the identification of k with some physical parameter. At this stage there are two approaches in the literature:

1. $k(r)$ is a modified proper distance, which leads to the Bonanno-Reuter metric [6]
2. $k(r) = \alpha K^{-1/4}$, where K is the Kretschmann scalar and $\alpha = 48^{-1/4}$ [4, 7, 9]), leading to the Held-Gold-Eichhorn metric, coinciding, up to the redefinition of constants, with the Hayward metric [10].

The metric of a spherically-symmetric black hole has the following general form

$$ds^2 = -f(r)dt^2 + f(r)^{-1}dr^2 + r^2 d\Omega^2, \quad (4)$$

with the only difference that now the Newton's "constant" depends on r .

The metric function for the Bonanno-Reuter identification (supposing that in the classical limit $G_0 = 1$) has the form

$$f(r) = 1 - \frac{2Mr^2}{r^3 + \frac{118}{15\pi}(r + \frac{9}{2}M)}, \quad (5)$$

where M is the black hole mass, measured in units of the Planck mass,

$$m_P \equiv \sqrt{\hbar c/G_0} \approx 2.176 \times 10^{-8} kg \approx 1.6 \times 10^{-35} m.$$

The event horizon exists when $M \geq M_{\text{crit}}$, where

$$\frac{M_{\text{crit}}}{m_P} = \frac{23\sqrt{5} + 5\sqrt{221}}{720} \sqrt{\frac{59}{3\pi} (31 + \sqrt{1105})} \approx 3.503.$$

The Held-Gold-Eichhorn metric function has the form:

$$f(r) = 1 - \frac{2r^2/M^2}{r^3/M^3 + \gamma}, \quad (6)$$

where the event horizon exists whenever $\gamma \leq 32/27$.

III. THE WAVE-LIKE EQUATIONS

The general covariant equations for the scalar field Φ , the electromagnetic field A_μ , and the Dirac field Υ [45] are respectively written as:

$$\frac{1}{\sqrt{-g}} \partial_\mu (\sqrt{-g} g^{\mu\nu} \partial_\nu \Phi) = 0, \quad (7a)$$

$$\frac{1}{\sqrt{-g}} \partial_\mu (F_{\rho\sigma} g^{\rho\nu} g^{\sigma\mu} \sqrt{-g}) = 0, \quad (7b)$$

$$\gamma^\alpha \left(\frac{\partial}{\partial x^\alpha} - \Gamma_\alpha \right) \Upsilon = 0, \quad (7c)$$

where $F_{\mu\nu} = \partial_\mu A_\nu - \partial_\nu A_\mu$ is the electromagnetic tensor, γ^α are noncommutative gamma matrices and Γ_α are spin connections in the tetrad formalism. After separation of the variables equations (7) take the Schrödinger-like form (see, for instance, [14, 15] and references therein)

$$\frac{d^2 \Psi}{dr_*^2} + (\omega^2 - V(r)) \Psi = 0, \quad (8)$$

where the "tortoise coordinate" r_* is defined by the following relation

$$dr_* \equiv \frac{dr}{f(r)}. \quad (9)$$

The effective potentials for the scalar ($s = 0$) and electromagnetic ($s = 1$) fields are

$$V(r) = f(r) \frac{\ell(\ell+1)}{r^2} + (1-s) \cdot \frac{f(r)}{r} \frac{df(r)}{dr}, \quad (10)$$

where $\ell = s, s+1, s+2, \dots$ are the multipole numbers. For the Dirac field we have two iso-spectral potentials

$$V_\pm(r) = W^2 \pm \frac{dW}{dr_*}, \quad W \equiv k \frac{\sqrt{f(r)}}{r}, \quad (11)$$

where $k = \ell + 1/2 = 1, 2, 3, \dots$ are the multipole numbers. The iso-spectral wave functions can be transformed one into another by the Darboux transformation

$$\Psi_+ = q \left(W + \frac{d}{dr_*} \right) \Psi_-, \quad q = \text{const}. \quad (12)$$

Therefore, we will calculate quasinormal modes for only one of the effective potentials, $V_+(r)$, because the WKB method works better for it.

IV. METHODS USED FOR CALCULATIONS OF QUASINORMAL MODES

Quasinormal modes ω_n are proper oscillation frequencies corresponding to the solutions of the master wave equation (8) when the purely outgoing waves at both infinities are imposed:

$$\Psi \propto e^{-i\omega t \pm i\omega r_*}, \quad r_* \rightarrow \pm\infty. \quad (13)$$

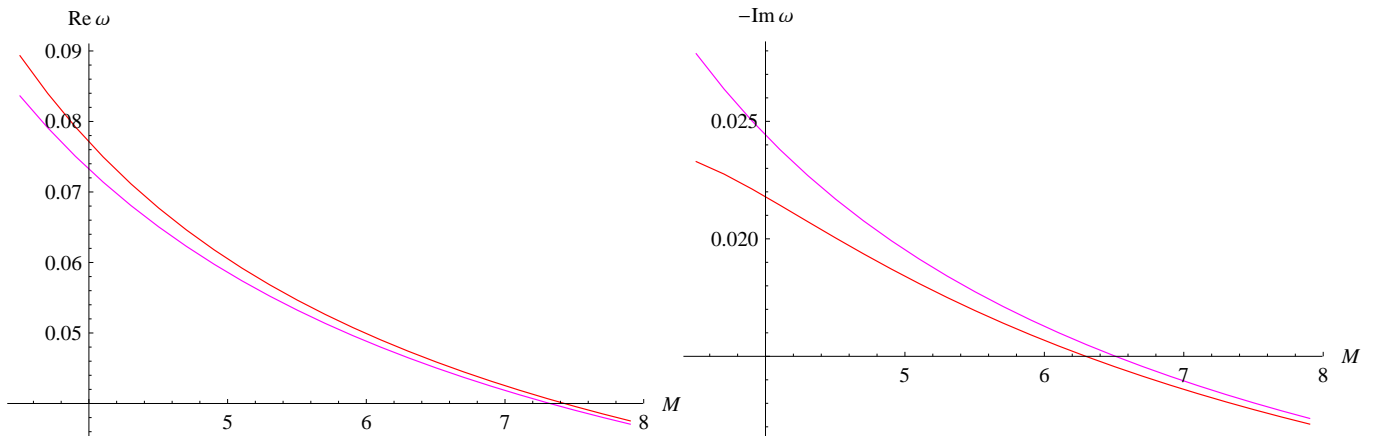


FIG. 1. The fundamental ($n = 0$) quasinormal modes of the Bonanno-Reuter black hole model (red) versus Schwarzschild modes (magenta) with the same mass for $\ell = 1$ scalar perturbations computed by the WKB method. The Schwarzschild mode has lower $Re(\omega)$ and higher decay rate.

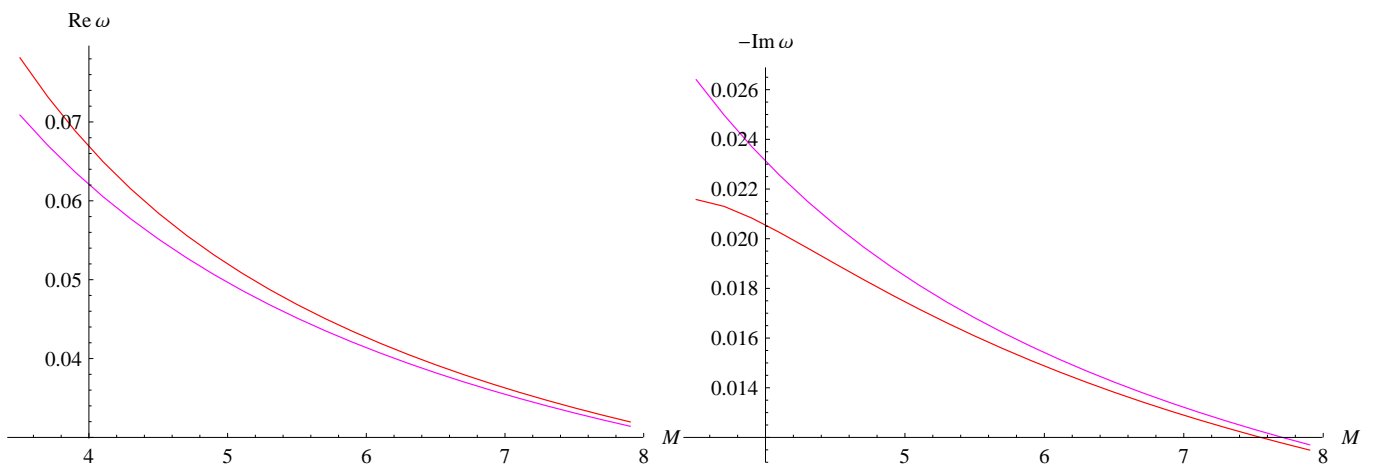


FIG. 2. The fundamental ($n = 0$) quasinormal modes of the Bonanno-Reuter black hole model (red) versus Schwarzschild modes (magenta) with the same mass for $\ell = 1$ electromagnetic perturbations computed by the WKB method. The Schwarzschild mode has lower $Re(\omega)$ and higher decay rate.

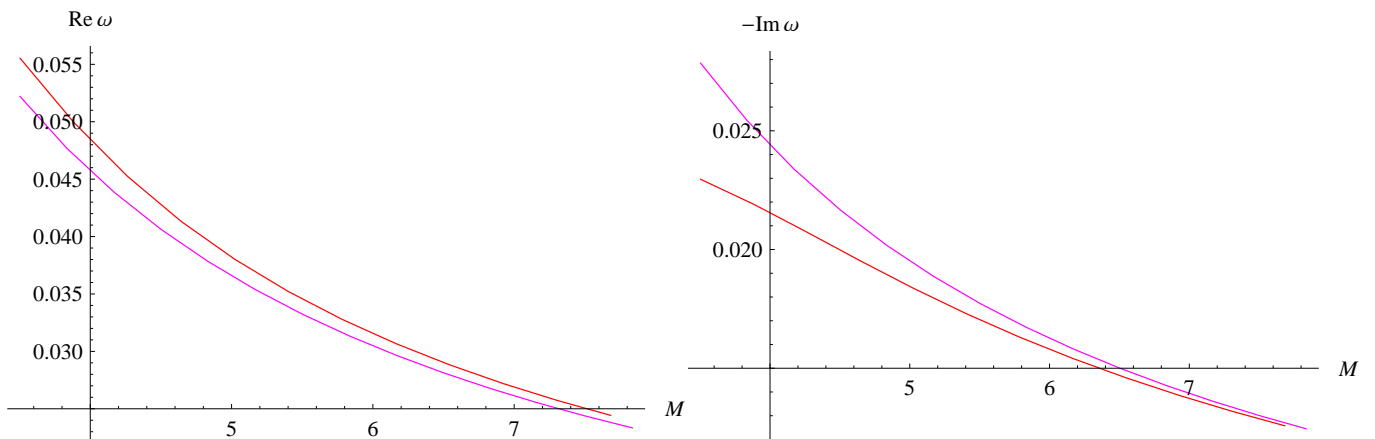


FIG. 3. The fundamental ($n = 0$) quasinormal modes of the Bonanno-Reuter black hole model (red) versus Schwarzschild modes (magenta) with the same mass for $\ell = 1/2$ Dirac perturbations computed by the WKB method. The Schwarzschild mode has lower $Re(\omega)$ and higher decay rate.

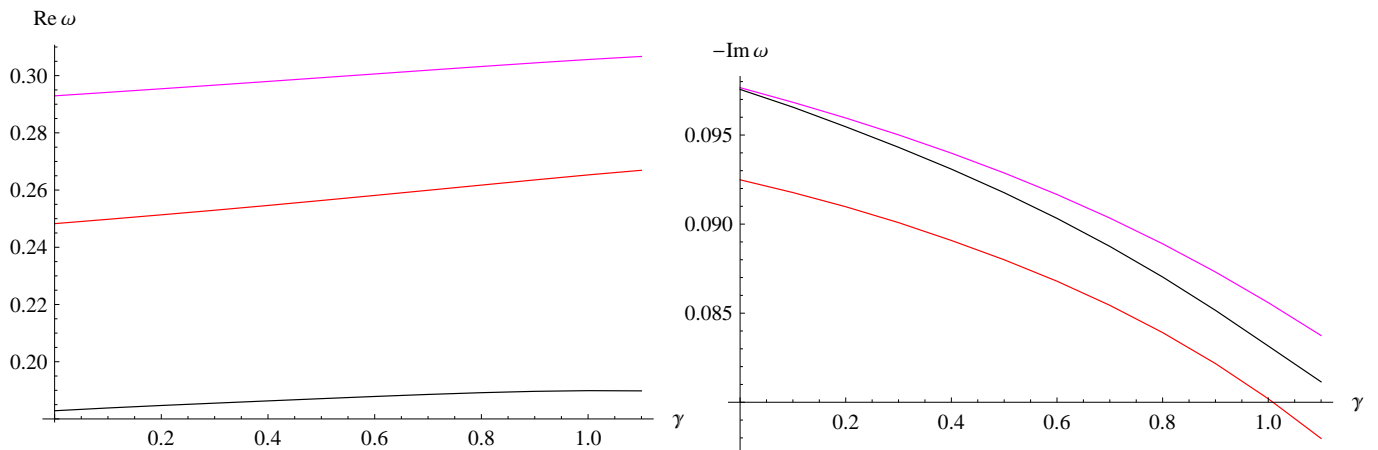


FIG. 4. The fundamental ($n = 0$) quasinormal modes of the Held-Gold-Eichhorn black hole model for $\ell = 1$ scalar (magenta, upper) and electromagnetic (red, lower imaginary part) perturbations, and $\ell = 1/2$ Dirac (black, lower real part) perturbations computed by the WKB method.

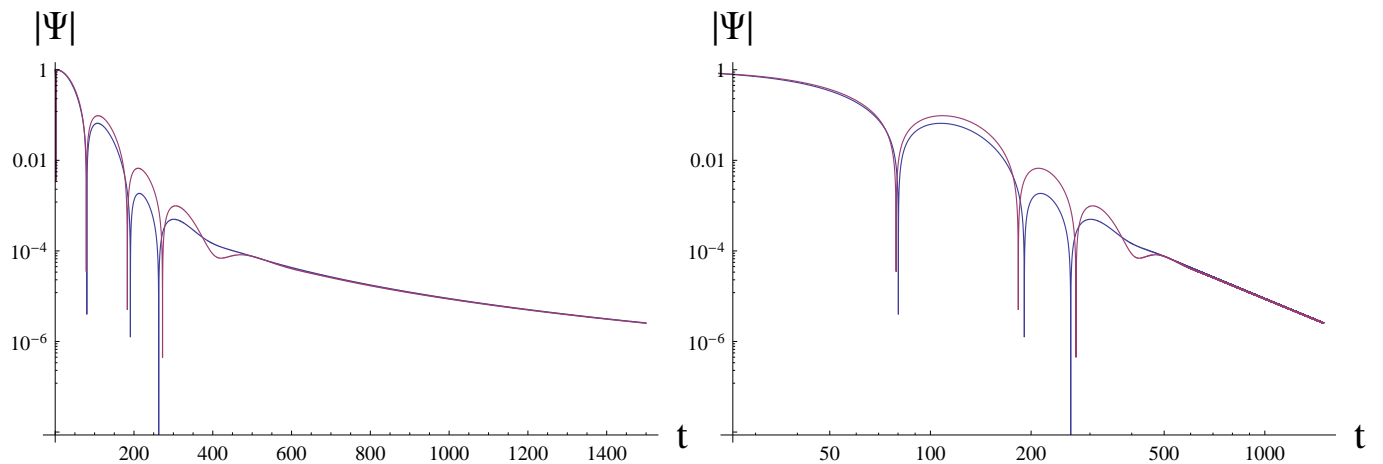


FIG. 5. Time-domain profile of $\ell = 0$ scalar perturbations of the Bonanno-Reuter (magenta, upper) and Schwarzschild (blue, lower) black holes, $M = 3.56$: Left panel - semi-logarithmic plot, right panel - logarithmic plot.

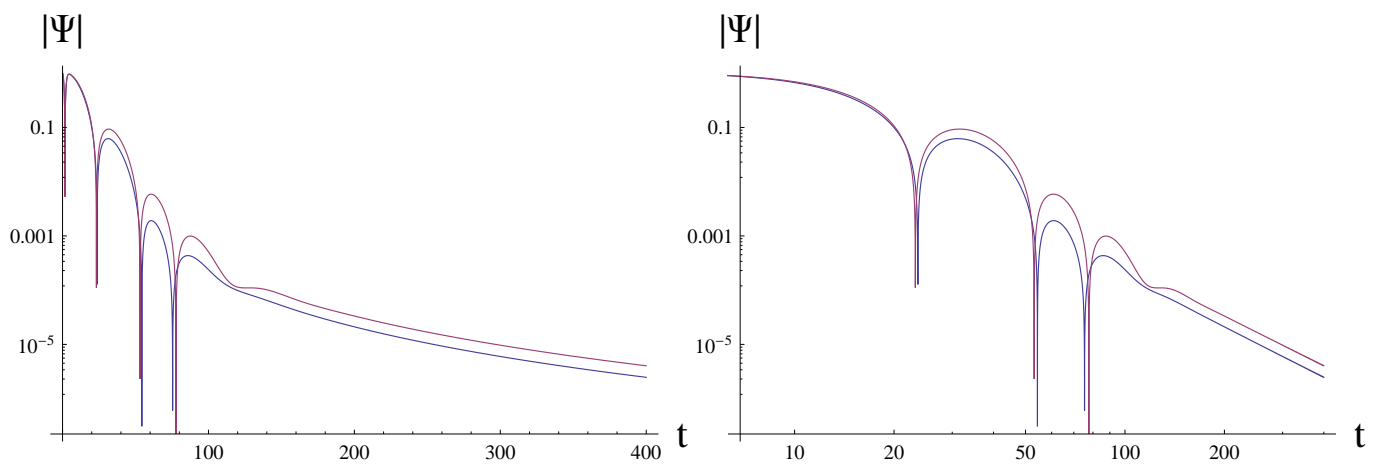


FIG. 6. Time-domain profile of $\ell = 0$ scalar perturbations of the Held-Gold-Eichhorn (magenta, upper) and Schwarzschild (blue, lower) black holes, $\gamma = 32/27$: Left panel - semi-logarithmic plot, right panel - logarithmic plot.

Thus, there are no waves coming from either infinity or the event horizon. Here we will review the three methods (time-domain integration, WKB, and Frobenius) used for calculations of quasinormal frequencies.

A. Time-domain integration

In order to find quasinormal modes and, foremost, analyze possible echo-like phenomena we will use the time-domain integration method. We will integrate the wavelike equation (8) in terms of the light-cone variables $u = t - r_*$ and $v = t + r_*$ via applying the discretization scheme of Gundlach-Price-Pullin [46],

$$\Psi(N) = \Psi(W) + \Psi(E) - \Psi(S) \quad (14)$$

$$- \Delta^2 V(S) \frac{\Psi(W) + \Psi(E)}{4} + \mathcal{O}(\Delta^4),$$

where the following notation for the points was used: $N \equiv (u + \Delta, v + \Delta)$, $W \equiv (u + \Delta, v)$, $E \equiv (u, v + \Delta)$, and $S \equiv (u, v)$. The Gaussian initial data are imposed on the two null surfaces, $u = u_0$ and $v = v_0$. The dominant quasinormal frequencies can be extracted from the time-domain profiles with the help of the Prony method see, e.g., [14].

B. WKB method

In the frequency domain we will use the semi-analytic WKB method applied by Will and Schutz [47] for finding quasinormal modes. The Will-Schutz formula was extended to higher orders in [48–50] and made even more accurate when using the Padé approximants in [50, 51]. The higher-order WKB formula has the form [52],

$$\omega^2 = V_0 + A_2(\mathcal{K}^2) + A_4(\mathcal{K}^2) + A_6(\mathcal{K}^2) + \dots \quad (15)$$

$$- i\mathcal{K}\sqrt{-2V_2}(1 + A_3(\mathcal{K}^2) + A_5(\mathcal{K}^2) + A_7(\mathcal{K}^2) + \dots),$$

where $\mathcal{K} = n + 1/2$ is half-integer. The corrections $A_k(\mathcal{K}^2)$ of the order k to the eikonal formula are polynomials of \mathcal{K}^2 with rational coefficients and depend on the values of higher derivatives of the potential $V(r)$ in its maximum. In order to increase accuracy of the WKB formula, we will follow the procedure of Matyjasek and Opala [50] and use the Padé approximants. Here we will use the sixth order WKB method with $\tilde{m} = 6$, where \tilde{m} is defined in [50, 52], because this choice provides the best accuracy in the Schwarzschild limit.

C. Frobenius method

In order to find the accurate values of QNMs we employ the method proposed by Leaver [53]. For the black holes of Bonanno-Reuter and Held-Gold-Eichhorn the wave-like equation (8) has regular singularities at the event

horizon $r = r_+$, the inner horizon $r = r_-$, and the irregular singularity at spatial infinity $r = \infty$. We introduce the new function,

$$\Psi(r) = e^{i\omega r} (r - r_-)^\lambda \left(\frac{r - r_+}{r - r_-} \right)^{-i\omega/f'(r_+)} y(r), \quad (16)$$

where λ is defined in such a way that $y(r)$ is regular at $r = \infty$ once $\Psi(r)$ corresponds to the purely outgoing wave at spatial infinity. We notice that $\Psi(r)$ behaves as the purely ingoing wave at the event horizon if $y(r)$ is regular at $r = r_+$. Therefore, we represent $y(r)$ in terms of the following Frobenius series:

$$y(r) = \sum_{k=0}^{\infty} a_k \left(\frac{r - r_+}{r - r_-} \right)^k, \quad (17)$$

and find that the coefficients a_k satisfy the 10-term recurrence relation, which can be reduced to the three-term recurrence relation via Gaussian elimination (see [14] for a detailed description of the procedure). Finally, using the recurrence relation coefficients, we find the equation with the infinite continued fraction with respect to ω , which is satisfied iff the series (17) converges at $r = \infty$, i.e., when $\Psi(r)$ obeys the quasinormal boundary conditions. In order to calculate the infinite continued fraction we use the Nollert improvement [54], which was generalized in [55] for an arbitrary number of terms in the recurrence relation.

V. QUASINORMAL FREQUENCIES AND TIME-DOMAIN PROFILES

Here we will use all the three above methods in order to find quasinormal modes. The fundamental mode can be found with sufficient accuracy by the WKB method and time-domain integration, while the overtones, specially those for which $n > \ell$, have been calculated with the Frobenius method.

From figs. 1, 2, and 3 one can see that the real oscillation frequency of the fundamental mode is larger for the Bonanno-Reuter black hole than for the Schwarzschild one with the same mass for scalar, electromagnetic, and Dirac fields. On the opposite, the damping rate is smaller than that of the Schwarzschild black hole. In the regime of large mass the quasinormal frequencies of the Bonanno-Reuter spacetime approach their Schwarzschild limit. In [38] it was claimed that the effect of the Bonanno-Reuter correction results in only a few percent difference from the Schwarzschild spectrum. However, there the minimal value of mass was taken $M = 5$, which is quite far from the extremal value $M \approx 3.503$. Here we extended the calculations to the extremal limit and found that, even for the fundamental mode, the effect is much larger than previously reported and exceeds 20 percent.

From fig. 4 we can see that the Held-Gold-Eichhorn black hole is characterized by qualitatively the same behavior of the fundamental mode: renormalization group

| M | ω (WKB) | ω (time-domain) | ω (accurate) | ω (Schwarzschild) |
|-------|------------------------------|------------------------------|------------------------------|------------------------------|
| 3.503 | 0.032153 - 0.025011 <i>i</i> | 0.032413 - 0.025440 <i>i</i> | 0.032094 - 0.025008 <i>i</i> | 0.031532 - 0.029945 <i>i</i> |
| 4.503 | 0.025774 - 0.021206 <i>i</i> | 0.025602 - 0.021954 <i>i</i> | 0.025759 - 0.021170 <i>i</i> | 0.024529 - 0.023295 <i>i</i> |
| 5.503 | 0.020744 - 0.018051 <i>i</i> | 0.019615 - 0.018257 <i>i</i> | 0.020820 - 0.018056 <i>i</i> | 0.020072 - 0.019062 <i>i</i> |
| 6.503 | 0.017421 - 0.015540 <i>i</i> | 0.016514 - 0.015338 <i>i</i> | 0.017450 - 0.015567 <i>i</i> | 0.016985 - 0.016130 <i>i</i> |
| 7.503 | 0.015030 - 0.013587 <i>i</i> | 0.014592 - 0.012703 <i>i</i> | 0.015027 - 0.013630 <i>i</i> | 0.014721 - 0.013981 <i>i</i> |
| 8.503 | 0.013216 - 0.012054 <i>i</i> | 0.012958 - 0.011343 <i>i</i> | 0.013201 - 0.012103 <i>i</i> | 0.012990 - 0.012336 <i>i</i> |
| 9.503 | 0.011793 - 0.010827 <i>i</i> | 0.011683 - 0.010191 <i>i</i> | 0.011775 - 0.010874 <i>i</i> | 0.011623 - 0.011038 <i>i</i> |

TABLE I. Fundamental quasinormal modes for the scalar $\ell = n = 0$ perturbations of the Bonanno-Reuter black hole.

| n | $\ell = 0$ | | $\ell = 1$ | |
|-----|------------------------------|------------------------------|------------------------------|------------------------------|
| | ω (Bonanno-Reuter) | ω (Schwarzschild) | ω (Bonanno-Reuter) | ω (Schwarzschild) |
| 0 | 0.029000 - 0.022799 <i>i</i> | 0.027614 - 0.026224 <i>i</i> | 0.077094 - 0.021791 <i>i</i> | 0.073234 - 0.024415 <i>i</i> |
| 1 | 0.014735 - 0.075427 <i>i</i> | 0.021529 - 0.087013 <i>i</i> | 0.070283 - 0.067061 <i>i</i> | 0.066112 - 0.076564 <i>i</i> |
| 2 | 0.013708 - 0.140628 <i>i</i> | 0.018936 - 0.150270 <i>i</i> | 0.058062 - 0.116660 <i>i</i> | 0.057385 - 0.135033 <i>i</i> |
| 3 | 0.006542 - 0.207654 <i>i</i> | 0.017603 - 0.213419 <i>i</i> | 0.043693 - 0.174315 <i>i</i> | 0.050815 - 0.197075 <i>i</i> |
| 4 | 0.006835 - 0.263913 <i>i</i> | 0.016769 - 0.276408 <i>i</i> | 0.031041 - 0.236051 <i>i</i> | 0.046277 - 0.260191 <i>i</i> |
| 5 | 0.004802 - 0.331462 <i>i</i> | 0.016185 - 0.339285 <i>i</i> | 0.025512 - 0.299442 <i>i</i> | 0.043019 - 0.323530 <i>i</i> |
| 6 | 0.001296 - 0.388573 <i>i</i> | 0.015749 - 0.402085 <i>i</i> | 0.019751 - 0.366931 <i>i</i> | 0.040557 - 0.386860 <i>i</i> |
| 7 | 0.002675 - 0.455550 <i>i</i> | 0.015405 - 0.464832 <i>i</i> | 0.008952 - 0.427228 <i>i</i> | 0.038614 - 0.450123 <i>i</i> |
| 8 | 0.00 - 0.51 <i>i</i> | 0.015127 - 0.527538 <i>i</i> | 0.012764 - 0.492353 <i>i</i> | 0.037032 - 0.513309 <i>i</i> |
| 9 | 0.001631 - 0.579538 <i>i</i> | 0.014894 - 0.590215 <i>i</i> | 0.008551 - 0.560693 <i>i</i> | 0.035709 - 0.576425 <i>i</i> |

TABLE II. Dominant quasinormal modes for the scalar perturbations of the Bonanno-Reuter black hole ($M = 4$) and the corresponding modes for the Schwarzschild black hole.

| n | ω (Bonanno-Reuter) | ω (Schwarzschild) |
|-----|------------------------------|------------------------------|
| 0 | 0.066877 - 0.020549 <i>i</i> | 0.062066 - 0.023122 <i>i</i> |
| 1 | 0.059764 - 0.063499 <i>i</i> | 0.053629 - 0.073417 <i>i</i> |
| 2 | 0.047392 - 0.110619 <i>i</i> | 0.043693 - 0.131297 <i>i</i> |
| 3 | 0.030448 - 0.166115 <i>i</i> | 0.036544 - 0.192977 <i>i</i> |
| 4 | 0.019951 - 0.224263 <i>i</i> | 0.031639 - 0.255638 <i>i</i> |
| 5 | 0.012209 - 0.290487 <i>i</i> | 0.028063 - 0.318481 <i>i</i> |
| 6 | 0.000983 - 0.354117 <i>i</i> | 0.025304 - 0.381317 <i>i</i> |
| 7 | 0.000 - 0.420 <i>i</i> | 0.023081 - 0.444100 <i>i</i> |

TABLE III. Dominant quasinormal modes for the electromagnetic perturbations ($\ell = 1$) of the Bonanno-Reuter black hole ($M = 4$) and the corresponding modes for the Schwarzschild black hole.

correction leads to higher real oscillation frequency and slower decay. Exception from such monotonic behavior occurs only for the $\ell = 0$ scalar field perturbation at $\gamma \approx 20/27$ for the fundamental mode (see table V). Overall, we can conclude that the quality factor of the corrected black hole is higher in both cases, that is, a black hole in the asymptotically safe gravity is a much better oscillator than its classical limit.

Comparison of the WKB data with the time-domain integration and Frobenius method (see tables I, II, and V) shows excellent concordance in the whole range of parameters. The Frobenius method is accurate, because it is

| n | ω (Bonanno-Reuter) | ω (Schwarzschild) |
|-----|------------------------------|------------------------------|
| 0 | 0.014060 - 0.012828 <i>i</i> | 0.013807 - 0.013112 <i>i</i> |
| 1 | 0.011030 - 0.042326 <i>i</i> | 0.010765 - 0.043507 <i>i</i> |
| 2 | 0.009447 - 0.073078 <i>i</i> | 0.009468 - 0.075135 <i>i</i> |
| 3 | 0.008318 - 0.103855 <i>i</i> | 0.008801 - 0.106710 <i>i</i> |
| 4 | 0.007282 - 0.134637 <i>i</i> | 0.008384 - 0.138204 <i>i</i> |
| 5 | 0.006213 - 0.165471 <i>i</i> | 0.008093 - 0.169642 <i>i</i> |
| 6 | 0.005055 - 0.196409 <i>i</i> | 0.007874 - 0.201043 <i>i</i> |
| 7 | 0.003780 - 0.227529 <i>i</i> | 0.007703 - 0.232416 <i>i</i> |
| 8 | 0.002403 - 0.258950 <i>i</i> | 0.007563 - 0.263769 <i>i</i> |
| 9 | 0.001041 - 0.290822 <i>i</i> | 0.007447 - 0.295107 <i>i</i> |
| 10 | 0.000042 - 0.323183 <i>i</i> | 0.007348 - 0.326434 <i>i</i> |
| 11 | 0.000000 - 0.355670 <i>i</i> | 0.007263 - 0.357751 <i>i</i> |
| 12 | 0.000000 - 0.387832 <i>i</i> | 0.007189 - 0.389061 <i>i</i> |
| 13 | 0.000091 - 0.419620 <i>i</i> | 0.007123 - 0.420364 <i>i</i> |
| 14 | 0.000279 - 0.451184 <i>i</i> | 0.007064 - 0.451662 <i>i</i> |
| 15 | 0.000389 - 0.482640 <i>i</i> | 0.007011 - 0.482956 <i>i</i> |

TABLE IV. Dominant quasinormal modes for the scalar $\ell = 0$ perturbations of the Bonanno-Reuter black hole ($M = 8$) and the corresponding modes for the Schwarzschild black hole.

based on the convergent procedure. This means that it is the criterium of accuracy for the other two methods and consequently both the time-domain integration and the WKB formula provide reasonable accuracy at least for

| γ | ωM (WKB) | ωM (time-domain) | ωM (accurate) |
|----------|------------------------------|------------------------------|------------------------------|
| 0 | 0.110678 - 0.104424 <i>i</i> | 0.110302 - 0.104679 <i>i</i> | 0.110455 - 0.104896 <i>i</i> |
| 4/27 | 0.111758 - 0.102964 <i>i</i> | 0.111477 - 0.103216 <i>i</i> | 0.111600 - 0.103409 <i>i</i> |
| 8/27 | 0.112523 - 0.101495 <i>i</i> | 0.112587 - 0.101530 <i>i</i> | 0.112698 - 0.101699 <i>i</i> |
| 12/27 | 0.113241 - 0.099667 <i>i</i> | 0.113603 - 0.099566 <i>i</i> | 0.113698 - 0.099717 <i>i</i> |
| 16/27 | 0.114205 - 0.097505 <i>i</i> | 0.114433 - 0.097266 <i>i</i> | 0.114512 - 0.097400 <i>i</i> |
| 20/27 | 0.115207 - 0.094804 <i>i</i> | 0.114902 - 0.094560 <i>i</i> | 0.114963 - 0.094678 <i>i</i> |
| 24/27 | 0.115156 - 0.091203 <i>i</i> | 0.114630 - 0.091441 <i>i</i> | 0.114675 - 0.091539 <i>i</i> |
| 28/27 | 0.112802 - 0.088751 <i>i</i> | 0.112802 - 0.088445 <i>i</i> | 0.112827 - 0.088526 <i>i</i> |
| 32/27 | 0.110844 - 0.087919 <i>i</i> | 0.110664 - 0.087749 <i>i</i> | |

TABLE V. Fundamental quasinormal modes for the scalar $\ell = n = 0$ perturbations of the Held-Gold-Eichhorn black hole.

| n | $\ell = 0$ | | $\ell = 1$ | |
|-----|---------------------------------|------------------------------|---------------------------------|------------------------------|
| | ωM (Held-Gold-Eichhorn) | ωM (Schwarzschild) | ωM (Held-Gold-Eichhorn) | ωM (Schwarzschild) |
| 0 | 0.113494 - 0.089160 <i>i</i> | 0.110455 - 0.104896 <i>i</i> | 0.305627 - 0.085590 <i>i</i> | 0.292936 - 0.097660 <i>i</i> |
| 1 | 0.066731 - 0.319873 <i>i</i> | 0.086117 - 0.348053 <i>i</i> | 0.274844 - 0.263717 <i>i</i> | 0.264449 - 0.306258 <i>i</i> |
| 2 | 0.041068 - 0.576924 <i>i</i> | 0.075742 - 0.601079 <i>i</i> | 0.218494 - 0.464862 <i>i</i> | 0.229540 - 0.540134 <i>i</i> |
| 3 | 0.021679 - 0.833067 <i>i</i> | 0.070410 - 0.853678 <i>i</i> | 0.158106 - 0.700610 <i>i</i> | 0.203259 - 0.788298 <i>i</i> |
| 4 | 0.000000 - 1.082236 <i>i</i> | 0.067074 - 1.105630 <i>i</i> | 0.112793 - 0.957178 <i>i</i> | 0.185109 - 1.040762 <i>i</i> |
| 5 | 0.001449 - 1.317232 <i>i</i> | 0.064742 - 1.357140 <i>i</i> | 0.081256 - 1.220106 <i>i</i> | 0.172077 - 1.294120 <i>i</i> |

TABLE VI. Quasinormal modes for the scalar perturbations of the Held-Gold-Eichhorn black hole ($\gamma = 1$) and the corresponding modes for the Schwarzschild black hole.

| n | ωM (Held-Gold-Eichhorn) | ωM (Schwarzschild) |
|-----|---------------------------------|------------------------------|
| 0 | 0.265285 - 0.080169 <i>i</i> | 0.248264 - 0.092488 <i>i</i> |
| 1 | 0.233370 - 0.247397 <i>i</i> | 0.214516 - 0.293668 <i>i</i> |
| 2 | 0.172918 - 0.437335 <i>i</i> | 0.174774 - 0.525188 <i>i</i> |
| 3 | 0.105275 - 0.663349 <i>i</i> | 0.146177 - 0.771909 <i>i</i> |
| 4 | 0.052269 - 0.905784 <i>i</i> | 0.126554 - 1.022551 <i>i</i> |
| 5 | 0.015138 - 1.152384 <i>i</i> | 0.112253 - 1.273926 <i>i</i> |
| 6 | 0.000 - 1.441 <i>i</i> | 0.101215 - 1.525267 <i>i</i> |

TABLE VII. Dominant quasinormal modes for the electromagnetic perturbations ($\ell = 1$) of the Held-Gold-Eichhorn black hole ($\gamma = 1$) and the corresponding modes for the Schwarzschild black hole.

the fundamental mode. For the near extreme Held-Gold-Eichhorn black hole the Frobenius method converges very slowly, so that the extremal limit in table V is calculated only by the time-domain integration and WKB methods.

Using the first order WKB formula we can obtain quasinormal modes in the high multipole number $\ell \rightarrow \infty$ regime in analytic form. For this we will use the expression for the position of the peak of the effective potential, which for the Bonanno-Reuter metric is located at:

$$r_{max} = 3M - \frac{1652}{135\pi M} - \frac{5071817}{54675\pi^2 M^3} - \frac{28261793432}{22143375\pi^3 M^5} - \frac{64480973421931}{2989355625\pi^4 M^7}. \quad (18)$$

Then, the WKB formula yields

$$Im(\omega) = \frac{(n + \frac{1}{2})}{3\sqrt{3}M} \left(1 - \frac{1298}{405\pi M^2} + \mathcal{O}\left(\frac{1}{M^4}\right) \right), \quad (19)$$

$$Re(\omega) = \frac{(\ell + \frac{1}{2})}{3\sqrt{3}M} \left(1 + \frac{59}{27\pi M^2} + \mathcal{O}\left(\frac{1}{M^4}\right) \right). \quad (20)$$

The same procedure for the Held-Gold-Eichhorn metric leads to the following expressions for the maximum of the potential and eikonal quasinormal modes:

$$r_{max} = 3M - \frac{2\gamma M}{9} - \frac{\gamma^2 M}{27} - \frac{70\gamma^3 M}{6561} - \frac{665\gamma^4 M}{177147}, \quad (21)$$

$$Im(\omega) = \frac{(n + \frac{1}{2})}{3\sqrt{3}M} \left(1 - \frac{2}{27}\gamma + \mathcal{O}(\gamma^2) \right), \quad (22)$$

$$Re(\omega) = \frac{(\ell + \frac{1}{2})}{3\sqrt{3}M} \left(1 - \frac{2}{54}\gamma + \mathcal{O}(\gamma^2) \right). \quad (23)$$

Notice, that according to [56] there is a correspondence between eikonal quasinormal modes of test fields and characteristics of null geodesics: The real and imaginary parts of ω are multiples of the frequency and instability timescale of the circular null geodesics respectively. This correspondence, however, is not guaranteed for gravitational and other non-minimally coupled fields [57, 58].

From figs. 5 and 6 we can see time-domain profiles of evolution of perturbations for the Bonanno-Reuter and Held-Gold-Eichhorn metrics in comparison with that for the Schwarzschild solution. While the initial period of

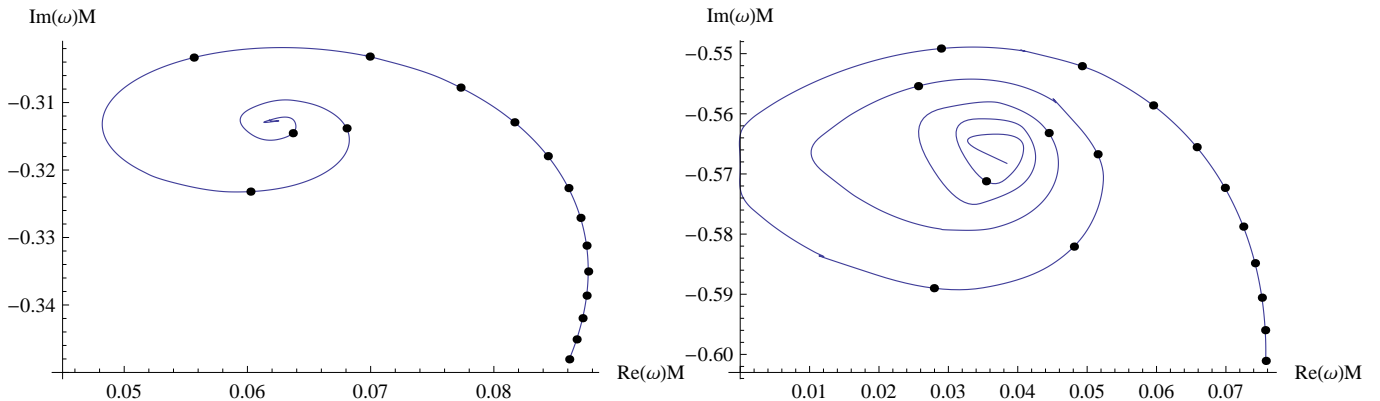


FIG. 7. First ($n = 1$) and second ($n = 2$) overtones of $\ell = 0$ scalar perturbations of the Held-Gold-Eichhorn black holes parametrized by γ : The black dots correspond to $27\gamma = 0, 2, 4, \dots, 30$ (from the bottom right corner, corresponding to the Schwarzschild mode, to the center of the spiral-like curve). For the parameters $0.702 \lesssim \gamma \lesssim 0.705$, the real part of the second overtone (right panel) becomes close to zero. The real part of the first overtone (left panel) is nonzero for all values of γ .

quasinormal ringing is characterized by relatively close fundamental quasinormal modes for both Schwarzschild and the corresponding corrected Schwarzschild-like metric, with time the initial phase is changed and the profiles do not merge. At asymptotically late times quasinormal modes are suppressed by the power-law tails which are the same as for the Schwarzschild case. Thus, for example, for the scalar perturbations shown on the above figures we have:

$$\Psi \propto t^{-(2\ell+3)}, \quad t \rightarrow \infty. \quad (24)$$

The tails in fig. 5 almost merge, because the geometries of the Schwarzschild and Bonanno-Reuter metrics are almost indistinguishable in the regime of large mass M chosen there. On the contrary, tails are parallel, but do not merge in fig. 6, because the parameter γ there is fixed to its extreme value and the deviation from the Schwarzschild metric is large.

The most striking difference occurs not at the fundamental mode, but at the overtones. First of all, for the Bonanno-Reuter black hole we have observed that the overtones differ from the Schwarzschild spectrum more than the fundamental mode: The real part of the higher overtones is much smaller than the corresponding mode of the Schwarzschild black hole. Second, we have found a purely imaginary mode for both test scalar $\ell = 0$, $n = 7$ (see table II and electromagnetic $\ell = 1$, $n = 6$ (table III) fields when $M = 4$. At larger mass, this non-oscillatory mode moves to higher overtones, being already $n = 11$ mode for $M = 8$. Notice, that the next overtone $n = 12$ is also purely imaginary at least within the numerical precision of 6 decimal places. Thus, in general there are more than one purely imaginary mode. When the mass is further increased, the purely imaginary modes move to even higher overtone number and simply disappear from the spectrum in the Schwarzschild limit. For the larger multipole we observe qualitatively the same effect: the real part rapidly decreases with the overtone number.

However, since the real part grows with the multipole number, the purely imaginary mode usually occurs at larger overtones.

The scalar and electromagnetic fields in the Held-Gold-Eichhorn background show a similar behavior: The real part of the overtones is suppressed as compared to the Schwarzschild black hole, and the non-oscillatory purely (or almost purely) damped modes appear in the spectra of the test fields. For $\gamma = 1$ the purely imaginary modes are $\ell = 0$, $n = 4$ for the scalar field (table VI) and $\ell = 1$, $n = 6$ for the electromagnetic field (table VII). The overtones' behavior for the Held-Gold-Eichhorn black hole is illustrated in fig. 7. One can see that, unlike the dominant mode (see table V), the first overtone as a function of γ goes along a spiral-like curve, though within a bounded region, such that only the real part changes significantly (within about 50% of the Schwarzschild value). For the second overtone the spiraling occurs faster as γ grows and the real part vanishes for some values of γ . Thus, one can observe the non-oscillating modes already at the second overtone.

We know that the algebraically special mode of the Schwarzschild black hole occurs at the 8-th overtone for gravitational perturbation [59]. On the contrary for both regular black holes considered here, the purely imaginary mode appears in the spectrum of a scalar field. To the best of our knowledge such purely imaginary modes at low overtones is not usual for asymptotically flat black holes, unlike the asymptotically AdS ones (see for instance [60–63] and references therein). One certainly needs to study these purely imaginary modes analytically in order to tell the purely imaginary mode from the mode with a very small real part, and to learn whether they belong to the class of algebraically special modes or not. Unfortunately, the Frobenius method apparently does not answer this question, because the convergence becomes slow when approaching purely imaginary modes. This is also a reason why we were able to calculate only

the first couple of significant digits for such modes. However, we have checked the results with the Bernstein spectral method code [64], which is particularly useful for finding purely imaginary modes. By comparing with the higher-order expansion in Bernstein polynomials we find that the error of the method is much larger than the usual error for the purely imaginary modes, indicating that the overtones have very small but nonzero real parts.

Another interesting feature of the overtones' behavior can be observed if we compare the real parts of overtones with those for the Schwarzschild case. In the regime when the deviation from the Schwarzschild geometry is tiny, that is, for large mass M for the Bonanno-Reuter metric and small γ for the Held-Gold-Eichhorn metric, the fundamental mode naturally differs from the Schwarzschild one insignificantly. However, for the same values of the parameters overtones deviate from their Schwarzschild analogues by hundreds of percent, leaving aside appearance of the purely imaginary modes. We believe that this happens because the overtones are sensitive to the near horizon asymptotic behavior, which is quite different, even once the metrics almost coincide with the Schwarzschild one farther from the horizon. Indeed, it is well-known that the limit $n \rightarrow \infty$ is crucially dependent on the event horizon asymptotic [65]. After all, the overtones are known to be sensitive to boundary conditions in the asymptotic regions as can be seen, for example, for the Schwarzschild-de Sitter black hole [66].

VI. CONCLUSIONS

Here we considered in detail quasinormal modes of scalar, electromagnetic, and Dirac fields in the background of two types of regular black holes in the asymptotically safe gravity: the Bonanno-Reuter and Held-Gold-Eichhorn metrics. We have found a number of peculiar features which were missed in the previous studies.

- The fundamental quasinormal modes are qualitatively similar for both types of identification, that is, the same behavior of the fundamental mode may

be appropriate to other ways of identification.

- The deviation of the fundamental mode from its Schwarzschild value for the Bonanno-Reuter metric can be more than twice larger than it was claimed in the previous studies.
- Unlike the fundamental mode, overtones are highly sensitive to even small deviation from the Schwarzschild limit, showing deviation of hundreds of percent already at the first few overtone. We believe that this feature may be quite general for various quantum corrected black holes, because the main difference with the classical solution is in the vicinity of the event horizon which is crucial for the overtones' behavior.
- There are purely imaginary (non-oscillatory) modes in the spectrum of both black holes, which may occur already at the second overtone.

Our work could be extended in a number of ways. In particular, the analysis of overtones could be done for other models of quantum corrected black hole metrics which are different from the Schwarzschild limit in the near horizon region, because the same high sensitivity of overtones to even tiny deformations of the geometry is expected in this case. Second, the nature of the purely imaginary mode should be studied: the appealing question is whether this mode is algebraically special or not. We hope that further studies will shed light on these questions.

ACKNOWLEDGMENTS

A. Z. was supported by Conselho Nacional de Desenvolvimento Científico e Tecnológico (CNPq). A. Z. thanks Institute of Physics of Silesian University in Opava for the hospitality. R. K. would like to acknowledge support of the grant 19-03950S of Czech Science Foundation (GAČR) and Institute of Physics of Oldenburg University for hospitality. J.K. would like to gratefully acknowledge support by the DFG Research Training Group 1620 *Models of Gravity* and the DFG project KU 612/18-1.

[1] A. Bonanno and M. Reuter. Cosmology with selfadjusting vacuum energy density from a renormalization group fixed point. *Phys. Lett. B*, 527:9–17, 2002.

[2] Alfio Bonanno and M. Reuter. Cosmological perturbations in renormalization group derived cosmologies. *Int. J. Mod. Phys. D*, 13:107–122, 2004.

[3] Claudio Rubano and Paolo Scudellaro. Variable G and λ : Scalar-tensor versus RG-improved cosmology. *Gen. Rel. Grav.*, 37:521–539, 2005.

[4] Jan M. Pawłowski and Dennis Stock. Quantum-improved Schwarzschild-(A)dS and Kerr-(A)dS spacetimes. *Phys.*

Rev. D, 98(10):106008, 2018.

[5] Benjamin Koch and Frank Saueressig. Structural aspects of asymptotically safe black holes. *Class. Quant. Grav.*, 31:015006, 2014.

[6] Alfio Bonanno and Martin Reuter. Renormalization group improved black hole space-times. *Phys. Rev.*, D62:043008, 2000.

[7] Aaron Held, Roman Gold, and Astrid Eichhorn. Asymptotic safety casts its shadow. *JCAP*, 06:029, 2019.

[8] Renata Ferrero and Martin Reuter. AdS/CFT and dS/CFT correspondences emerging from Asymptotic

- Safety ? 5 2022.
- [9] Alessia Platania. Dynamical renormalization of black-hole spacetimes. *Eur. Phys. J. C*, 79(6):470, 2019.
- [10] Sean A. Hayward. Formation and evaporation of regular black holes. *Phys. Rev. Lett.*, 96:031103, 2006.
- [11] D. I. Kazakov and S. N. Solodukhin. On Quantum deformation of the Schwarzschild solution. *Nucl. Phys.*, B429:153–176, 1994.
- [12] R. A. Konoplya. Quantum corrected black holes: quasinormal modes, scattering, shadows. *Phys. Lett. B*, 804:135363, 2020.
- [13] Mahamat Saleh, Bouetou Thomas Bouetou, and Timoleon Crepin Kofane. Quasinormal modes of a quantum-corrected Schwarzschild black hole: gravitational and Dirac perturbations. *Astrophys. Space Sci.*, 361(4):137, 2016.
- [14] R. A. Konoplya and A. Zhidenko. Quasinormal modes of black holes: From astrophysics to string theory. *Rev. Mod. Phys.*, 83:793–836, 2011.
- [15] Kostas D. Kokkotas and Bernd G. Schmidt. Quasinormal modes of stars and black holes. *Living Rev. Rel.*, 2:2, 1999.
- [16] B. P. Abbott et al. Observation of Gravitational Waves from a Binary Black Hole Merger. *Phys. Rev. Lett.*, 116(6):061102, 2016.
- [17] B. P. Abbott et al. GW151226: Observation of Gravitational Waves from a 22-Solar-Mass Binary Black Hole Coalescence. *Phys. Rev. Lett.*, 116(24):241103, 2016.
- [18] Benjamin P. Abbott et al. GW170104: Observation of a 50-Solar-Mass Binary Black Hole Coalescence at Redshift 0.2. *Phys. Rev. Lett.*, 118(22):221101, 2017. [Erratum: *Phys. Rev. Lett.* 121, no. 12, 129901 (2018)].
- [19] Roman Konoplya and Alexander Zhidenko. Detection of gravitational waves from black holes: Is there a window for alternative theories? *Phys. Lett. B*, 756:350–353, 2016.
- [20] K. A. Bronnikov, R. A. Konoplya, and A. Zhidenko. Instabilities of wormholes and regular black holes supported by a phantom scalar field. *Phys. Rev. D*, 86:024028, 2012.
- [21] L. A. López and Valeria Ramírez. Quasinormal modes of a Generic-class of magnetically charged regular black hole: scalar and electromagnetic perturbations. 5 2022.
- [22] Chen Lan and Yi-Fan Wang. Singularities of regular black holes and the art of monodromy method for asymptotic quasinormal modes. 5 2022.
- [23] Ángel Rincón and Victor Santos. Greybody factor and quasinormal modes of Regular Black Holes. *Eur. Phys. J. C*, 80(10):910, 2020.
- [24] Kimet Jusufi, Mustapha Azreg-Aïnou, Mubasher Jamil, Shao-Wen Wei, Qiang Wu, and Anzhong Wang. Quasinormal modes, quasiperiodic oscillations, and the shadow of rotating regular black holes in nonminimally coupled Einstein-Yang-Mills theory. *Phys. Rev. D*, 103(2):024013, 2021.
- [25] Chen Lan, Yan-Gang Miao, and Hao Yang. Quasinormal modes and phase transitions of regular black holes. *Nucl. Phys. B*, 971:115539, 2021.
- [26] S. H. Hendi, S. N. Sajadi, and M. Khademi. Physical properties of a regular rotating black hole: Thermodynamics, stability, and quasinormal modes. *Phys. Rev. D*, 103(6):064016, 2021.
- [27] Davood Mahdavian Yekta, Majid Karimabadi, and S. A. Alavi. Quasinormal modes for non-minimally coupled scalar fields in regular black hole spacetimes: Grey-body factors, area spectrum and shadow radius. *Annals Phys.*, 434:168603, 2021.
- [28] Grigoris Panotopoulos and Ángel Rincón. Quasinormal modes of regular black holes with non linear-Electrodynamical sources. *Eur. Phys. J. Plus*, 134(6):300, 2019.
- [29] Mahamat Saleh, Bouetou Bouetou Thomas, and Timoleon Crepin Kofane. Quasinormal modes of gravitational perturbation around regular Bardeen black hole surrounded by quintessence. *Eur. Phys. J. C*, 78(4):325, 2018.
- [30] Chen Wu. Quasinormal frequencies of gravitational perturbation in regular black hole spacetimes. *Eur. Phys. J. C*, 78(4):283, 2018.
- [31] Jin Li, Kai Lin, and Hao Wen. Gravitational Quasinormal Modes of Regular Phantom Black Hole. *Adv. High Energy Phys.*, 2017:5234214, 2017.
- [32] Sharmanthie Fernando. Regular black holes in de Sitter universe: scalar field perturbations and quasinormal modes. *Int. J. Mod. Phys. D*, 24(14):1550104, 2015.
- [33] Bobir Toshmatov, Ahmadjon Abdujabbarov, Zdeněk Stuchlík, and Bobomurat Ahmedov. Quasinormal modes of test fields around regular black holes. *Phys. Rev. D*, 91(8):083008, 2015.
- [34] Jin Li, Ma Hong, and Kai Lin. Dirac quasinormal modes in spherically symmetric regular black holes. *Phys. Rev. D*, 88:064001, 2013.
- [35] Kai Lin, Jin Li, and Shuzheng Yang. Quasinormal Modes of Hayward Regular Black Hole. *Int. J. Theor. Phys.*, 52:3771–3778, 2013.
- [36] Antonino Flachi and José P. S. Lemos. Quasinormal modes of regular black holes. *Phys. Rev. D*, 87(2):024034, 2013.
- [37] Poulami Dutta Roy and Sayan Kar. Generalised Hayward spacetimes: geometry, matter and scalar quasinormal modes. 6 2022.
- [38] Ángel Rincón and Grigoris Panotopoulos. Quasinormal modes of an improved Schwarzschild black hole. *Phys. Dark Univ.*, 30:100639, 2020.
- [39] Grigoris Panotopoulos and Ángel Rincón. Quasinormal spectra of scale-dependent Schwarzschild–de Sitter black holes. *Phys. Dark Univ.*, 31:100743, 2021.
- [40] Jin Li and Yuanhong Zhong. Quasinormal Modes for Electromagnetic Field Perturbation of the Asymptotic Safe Black Hole. *Int. J. Theor. Phys.*, 52:1583–1587, 2013.
- [41] Dao-Jun Liu, Bin Yang, Yong-Jia Zhai, and Xin-Zhou Li. Quasinormal modes for asymptotic safe black holes. *Class. Quant. Grav.*, 29:145009, 2012.
- [42] Matthew Giesler, Maximiliano Isi, Mark A. Scheel, and Saul Teukolsky. Black Hole Ringdown: The Importance of Overtones. *Phys. Rev. X*, 9(4):041060, 2019.
- [43] Naritaka Oshita. Ease of excitation of black hole ringing: Quantifying the importance of overtones by the excitation factors. *Phys. Rev. D*, 104(12):124032, 2021.
- [44] Xisco Jiménez Forteza and Pierre Mourier. High-overtone fits to numerical relativity ringdowns: Beyond the dismissed $n=8$ special tone. *Phys. Rev. D*, 104(12):124072, 2021.
- [45] Dieter R. Brill and John A. Wheeler. Interaction of neutrinos and gravitational fields. *Rev. Mod. Phys.*, 29:465–479, 1957.
- [46] Carsten Gundlach, Richard H. Price, and Jorge Pullin.

- Late time behavior of stellar collapse and explosions: 1. Linearized perturbations. *Phys. Rev. D*, 49:883–889, 1994.
- [47] Bernard F. Schutz and Clifford M. Will. Black hole normal modes: a semianalytic approach. *Astrophys. J. Lett.*, 291:L33–L36, 1985.
- [48] Sai Iyer and Clifford M. Will. Black Hole Normal Modes: A WKB Approach. 1. Foundations and Application of a Higher Order WKB Analysis of Potential Barrier Scattering. *Phys. Rev. D*, 35:3621, 1987.
- [49] R. A. Konoplya. Quasinormal behavior of the d -dimensional Schwarzschild black hole and higher order WKB approach. *Phys. Rev. D*, 68:024018, 2003.
- [50] Jerzy Matyjasek and Michał Opala. Quasinormal modes of black holes. The improved semianalytic approach. *Phys. Rev. D*, 96(2):024011, 2017.
- [51] Yasuyuki Hatsuda. Quasinormal modes of black holes and Borel summation. *Phys. Rev. D*, 101(2):024008, 2020.
- [52] R. A. Konoplya, A. Zhidenko, and A. F. Zinhailo. Higher order WKB formula for quasinormal modes and greybody factors: recipes for quick and accurate calculations. *Class. Quant. Grav.*, 36:155002, 2019.
- [53] E. W. Leaver. An Analytic representation for the quasinormal modes of Kerr black holes. *Proc. Roy. Soc. Lond. A*, 402:285–298, 1985.
- [54] Hans-Peter Nollert. Quasinormal modes of Schwarzschild black holes: The determination of quasinormal frequencies with very large imaginary parts. *Phys. Rev. D*, 47:5253–5258, 1993.
- [55] Alexander Zhidenko. Massive scalar field quasi-normal modes of higher dimensional black holes. *Phys. Rev. D*, 74:064017, 2006.
- [56] Vitor Cardoso, Alex S. Miranda, Emanuele Berti, Helvi Wittek, and Vilson T. Zanchin. Geodesic stability, Lyapunov exponents and quasinormal modes. *Phys. Rev. D*, 79(6):064016, 2009.
- [57] R. A. Konoplya and Z. Stuchlík. Are eikonal quasinormal modes linked to the unstable circular null geodesics? *Phys. Lett. B*, 771:597–602, 2017.
- [58] R. A. Konoplya, A. F. Zinhailo, and Z. Stuchlík. Quasinormal modes, scattering, and Hawking radiation in the vicinity of an Einstein-dilaton-Gauss-Bonnet black hole. *Phys. Rev. D*, 99(12):124042, 2019.
- [59] S. Chandrasekhar. The Mathematical Theory of Black Holes. *Fundam. Theor. Phys.*, 9:5–26, 1984.
- [60] Vitor Cardoso, Roman Konoplya, and Jose P. S. Lemos. Quasinormal frequencies of Schwarzschild black holes in anti-de Sitter space-times: A Complete study on the asymptotic behavior. *Phys. Rev. D*, 68:044024, 2003.
- [61] R. A. Konoplya and A. Zhidenko. Quasinormal modes of Gauss-Bonnet-AdS black holes: towards holographic description of finite coupling. *JHEP*, 09:139, 2017.
- [62] P. A. González, R. A. Konoplya, and Yerko Vásquez. Quasinormal modes of a scalar field in the Einstein-Gauss-Bonnet-AdS black hole background: Perturbative and nonperturbative branches. *Phys. Rev. D*, 95(12):124012, 2017.
- [63] Sašo Grozdanov, Pavel K. Kovtun, Andrei O. Starinets, and Petar Tadić. The complex life of hydrodynamic modes. *JHEP*, 11:097, 2019.
- [64] Sean Fortuna and Ian Vega. Bernstein spectral method for quasinormal modes and other eigenvalue problems. 3 2020.
- [65] Lubos Motl and Andrew Neitzke. Asymptotic black hole quasinormal frequencies. *Adv. Theor. Math. Phys.*, 7(2):307–330, 2003.
- [66] R. A. Konoplya and A. Zhidenko. High overtones of Schwarzschild-de Sitter quasinormal spectrum. *JHEP*, 06:037, 2004.